

The Antarctic climate anomaly and galactic cosmic rays

Henrik Svensmark

*Center for Sun Climate Research, Danish National Space Center,
Juliane Marie Vej 30, 2100 Copenhagen Ø, Denmark*

(Received)

It has been proposed that galactic cosmic rays may influence the Earth's climate by affecting cloud formation. If changes in cloudiness play a part in climate change, their effect changes sign in Antarctica. Satellite data from the Earth Radiation Budget Experiment (ERBE) are here used to calculate the changes in surface temperatures at all latitudes, due to small percentage changes in cloudiness. The results match the observed contrasts in temperature changes, globally and in Antarctica. Evidently clouds do not just respond passively to climate changes but take an active part in the forcing, in accordance with changes in the solar magnetic field that vary the cosmic-ray flux.

Evidence has accumulated in recent years that the influx of galactic cosmic rays, as modulated by solar magnetic activity, influences the Earth's temperature by varying the cloudiness at low altitudes[1, 2, 3]. Electrons liberated by muons help to make the cloud condensation nuclei on which water droplets form[4]. There is now no reason to doubt that the Earth's atmosphere acts like a natural cloud chamber that registers the passing muons. What remains to be demonstrated is that the resulting clouds affect the climate, and that is the purpose of this paper.

Contradictory trends in temperature in Antarctica and the rest of the world, which are evident on timescales from millennia to decades, provide a strong clue to what drives climate change. The southern continent is distinguished by its isolation and by its unusual response to changes in cloud cover. While the rest of the global surface is (on balance) cooled by clouds, they have a warming effect on high-albedo snowfields[5, 6, 7, 8, 9, 10]. NASA's Earth Radiation Budget Experiment (ERBE) [11, 12] provided valuable data on the effects of clouds at different latitudes. They can be interpreted to show that, if changes in cloudiness drive climate change, the anomalous behavior of Antarctica is predictable

Borehole temperatures in the ice sheets spanning the past 6000 years show Antarctica repeatedly warming when Greenland cooled, and vice versa (Fig. 1) [13, 14]. North-south oscillations of greater amplitude associated with Dansgaard-Oeschger events are evident in oxygen-isotope data from the Wurm-Wisconsin glaciation[15]. The phenomenon has been called the polar see-saw[15, 16], but that implies a north-south symmetry that is absent. Greenland is better coupled to global temperatures than Antarctica is, and the fulcrum of the temperature swings is near the Antarctic Circle. A more apt term for the effect is the Antarctic climate anomaly.

Attempts to account for it have included the hypothesis of a south-flowing warm ocean current crossing the Equator[17] with a built-in time lag supposedly intended to match paleoclimatic data. That there is no significant delay in the Antarctic climate anomaly is already

apparent at the high-frequency end of Fig. (1). While mechanisms involving ocean currents might help to intensify or reverse the effects of climate changes, they are too slow to explain the almost instantaneous operation of the Antarctic climate anomaly.

The contrasts in temperature trends are not predicted by variations in the concentrations of carbon dioxide and other greenhouse gases. These gases diffuse throughout the atmosphere as far as the South Pole. When they increase, climate models predict simultaneous and strong warming at both ends of the Earth. There is no direct physical reason why this forcing should operate differently in the two polar regions.

The simplest and most immediate explanation of the Antarctic climate anomaly comes from cloud forcing. In most climate models, clouds are passive participants responding to changes due to other forcing agents. If, on the other hand, changes in cloudiness and GCR's drive the Earth's climate[1, 2, 3] the Antarctic climate anomaly is the exception that proves the rule.

Clouds warm the underlying surface by trapping the outgoing long-wave radiation, and cool it by reflecting the short-wave radiation from the Sun. In general the cooling effect is greater than the heating effect, resulting in a net cooling of the Earth of the order of 15 W/m^2 . A small percentage change in cloud cover can therefore result in significant forcing.

The cooling effect is not evenly distributed. As shown in Fig. (2 a) it is minimal around the Equator and increases towards the mid-latitudes. In polar regions the clouds can have a warming effect if their re-radiation of long-wave energy downwards dominates over the loss of short-wave solar energy blocked by the clouds. This warming has been well recorded on the surface in both the Arctic and Antarctic[5, 6, 7, 8, 9, 10]

Figure (2a) also shows that the polar warming effect of clouds is not symmetrical, being most pronounced beyond 75°S . In the Arctic it does no more than offset the cooling effect, despite the fact that the Arctic is much cloudier than the Antarctic (Fig. (2b)). The main reason for the difference seems to be the exceptionally high

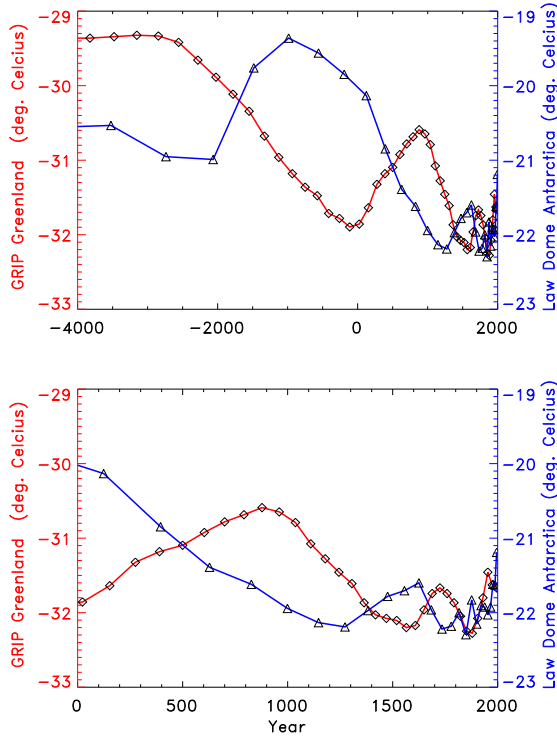


FIG. 1: Ice temperatures from the GRIP site in Greenland (73°N, 38°W)(red) and Law Dome in Antarctica (67°N, 112°E)(blue) using borehole thermometry data from Dahl-Jensen et al.[13, 14]. The Antarctic climate anomaly is particularly conspicuous during the cold period of the first millennium BC and the warm Viking Age c. 1000 AD. The apparent increase in frequency of the oscillations is not real but is due to a smoothing of the older temperature records by thermal conduction in the ice.

albedo of Antarctica in the absence of clouds.

The ERBE satellite data shown in Fig. (2) provide a basis for computing the cooling and warming effects of small changes in cloud cover. The changes are assumed to be the same at all latitudes. In order to achieve a forcing that is independent of cloud fraction, the net cloud forcing in Fig. (2) (a) is normalized with the cloud fraction in Fig. (2) (b) to derive the cloud forcing at different latitudes for a 1 % increase in cloud fraction, as shown in red in Fig. (2) (c). Finally, the blue curve in Fig. (2) (c) is a simplified version of the cloud forcing used as $(F_{\text{cloud}}(q))$ in the calculation that follows. A simple model balances incoming short-wave energy from the sun and outgoing long-wave radiation, and allows diffusion of heat between neighboring latitude bands. It takes the form[18]

$$c \partial_t U(x, t) = \partial_x (1 - x^2) D(x) \partial_x U(x, t) + QS(x)(1 - \alpha(x)) - A - BU(x, t) - \Delta_0 F_{\text{cloud}}(x) \quad (1)$$

where $x = \sin q$ and q is latitude. $U(x, t)$ is the temperature at latitude $x = \sin q$, t is time, c is the heat capacitance, $D(x)$ is an eddy diffusion constant that varies

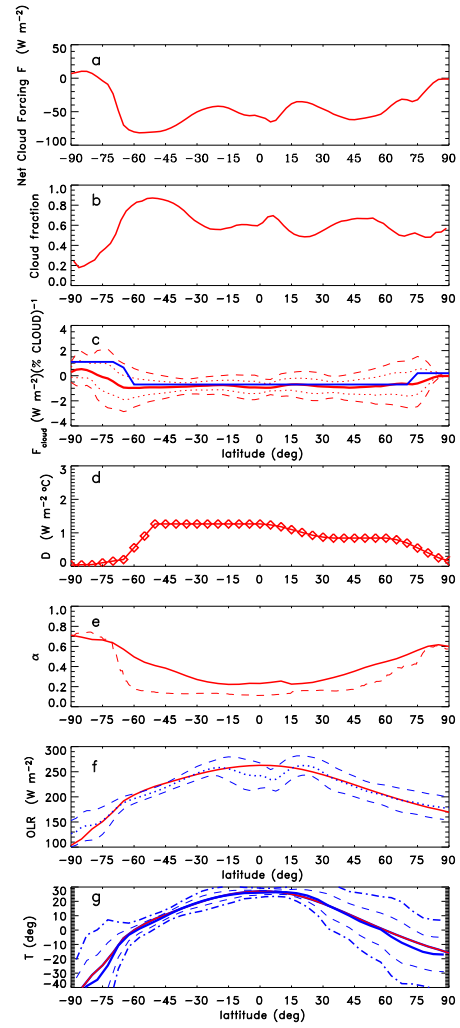


FIG. 2: Satellite observations (ERBE data [ref.]) relevant to calculations of the forcing effect of a change in cloudiness at different latitudes. a: Net cloud forcing by latitude. b: Cloud fraction by latitude. c: Net cloud forcing from a 1 % uniform change in cloud cover (red curve), together with one and two sigma variations (broken lines). The blue curve is the $F_{\text{cloud}}(q)$ function used in the model given by Eq. (1). Parametrization used in the model given by Eq. (1) as a function of latitude. d: Eddy-diffusion constant. e: Albedo solid red line. Broken red line is clear sky albedo. Finally the model Eq. (1) results compared with observations f: Out going long-wave radiation. Blue line observation based on ERBE with root mean square variances (dotted blue lines), red line model result. g: Observed surface temperatures solid blue with one and two sigma variations. Red curve model result.

with latitude and is shown in Fig. (2d), Q is the solar constant (1370 W/m^2), $S(x)$ is the average fraction of solar radiation at latitude x , and $\alpha(x)$ is the albedo at latitude x shown in Fig. (2e) solid red curve[12]. Δ_0 is the percentage change in cloud cover, compounded with $F_{\text{cloud}}(q)$ from Fig. (2) (c) The adjustable parameters A and B determine the long-wave loss at latitude q . The resulting values are $Q=1370 \text{ W/m}^2$, $A=215 \text{ W/m}^2$, and

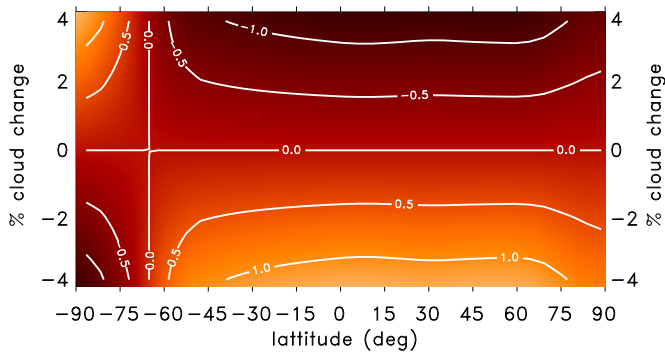


FIG. 3: Top panel: Calculated responses of surface temperatures at different latitudes to uniform percentage changes in cloud cover (Δ_0) from -4% to $+4\%$. The contour lines show temperature changes in fractions of a degree Celsius. Note the saddle-point of the Antarctic climate anomaly at latitude -63 .

$B = 1.7 \text{ W/m}^2\text{C}^{-1}$. Since Eq. (1) is solved for steady state the value of c is not important and was set to 1 numerically. The procedure used, was to adjust the eddy diffusion constant so both the model outgoing longwave radiation[11, 12] and the model surface temperature, as a function of latitude fitted observations[19]. The results of this procedure are shown in Fig. (2e) and Fig. (2g).

The calculated temperature changes in response to a uniform variation of the cloud cover are shown in Fig. (3). The sign of the response (warming or cooling) reverses at a saddle-point which in this simple model is around -63 deg. latitude. The climate sensitivity of the model is approximately $\gamma = 0.5 \text{ W}^{-1}\text{m}^2\text{C}$. For an $\pm 4\%$ change in cloud cover, the variation in temperature is about 2°C at $+80$ deg. and $\approx 1.5^\circ\text{C}$ (opposite sign) at -80 deg. Such changes can account for the temperature excursions of 2°C or less between Greenland and Antarctica during the past 6000 years, shown in Fig. (1).

Figure (3) also predicts that a reduction in cloud cover of about 8% is sufficient to warm most of the globe by almost 2°C , which is in line with other estimates of cloud forcing during the 20th Century[1]. The effect is seen in the upper curve of Fig. (4a) (NASA-GISS data[20]). In a cloud interpretation the hesitations and advances in cloud reduction since 1900 follow the well-known changes in solar activity[1, 21]. The lower curve in Fig. (4a) shows the corresponding changes in Antarctica, and the operation of the Antarctic climate anomaly is plain to see. Note especially the fall in Antarctic temperatures in the 1920s contrasting with a surge in global temperatures, and the marked rise 1950–70 when global temperatures fell.

Unfortunately there do not exist a record of cloud cover that could verify the connection between clouds and climate directly. However satellite data of Earths cloud cover from the International Satellite Cloud Climate Project (ISCCP) covering 1983 – 2005 show that

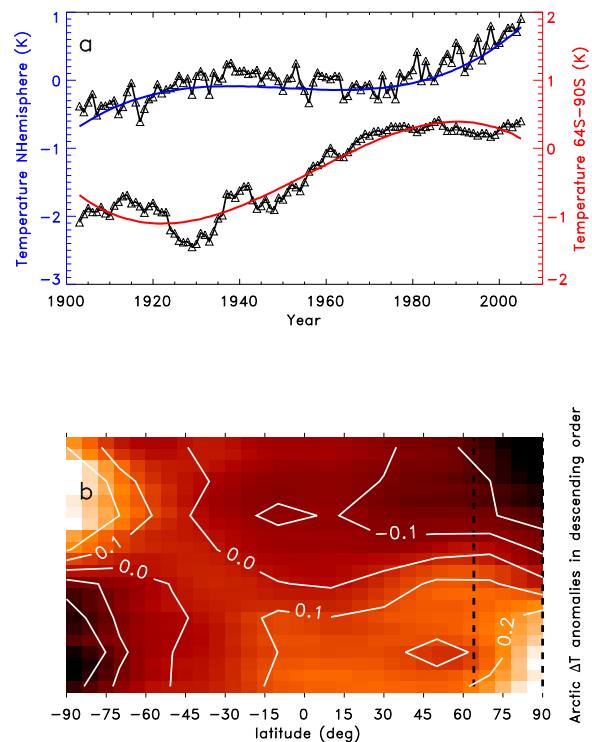


FIG. 4: **a**: The Antarctic climate anomaly during the past 100 years is apparent in this comparison of the annual surface temperature anomalies for the northern hemisphere and Antarctica (64S-90S), from the NASA-GISS compilations. The Antarctic data has been averaged over 12 years to minimize the temperature fluctuations. The blue and red line are fourth order polynomial fit to the northern hemisphere data and the Antarctica (64S-90S) data, respectively. If the two curves were not offset by 1°C , for clarity, the polynomial trendlines would cross and re-cross around 1910, 1955 and 1995, in the same manner as the millennial-scale curves of the Antarctic climate anomaly in Fig. 1. In the cloud-forcing picture, the overall warming of the Antarctic during the 20th Century is probably due to negative feedback from the greenhouse action of increasing water vapor reaching the polar atmosphere. **b**: Visualization of the Antarctic climate anomaly using the NASA-GISS compilations of annual temperature anomalies ΔT for 1903-2005 in 102 time intervals and 8 zonal bands ($\pm(90-64) \pm(64-44) \pm(44-24) \pm(24-0)$). First, the linear trend in each zonal time series is removed. Next, the data for the 102 time intervals in the Arctic series are arranged in descending order of ΔT on the right side of the figure, poleward of 64 deg, between the black dotted lines. Then the ΔT 's for the corresponding time intervals are plotted for each of the other zones. Finally the surface is smoothed and contour lines of ΔT in $^\circ\text{C}$ are added. Note the N-S contrast in every time interval, and the topological similarity to the computed cloud forcing in Fig. (3).

the large scale temporal variations are distributed fairly evenly over the globe[3], and for example cloud variations over oceans and clouds over Antarctica have similar temporal evolution.

A remaining question about Fig. (4a) is how the

Antarctic temperatures were dragged upwards, to take part in the general warming, despite the long-term reduction in cloud cover. A natural mechanism must be in operation, because similar correspondences (though in the context of an overall global cooling) are seen on the millennial scale in the Greenland and Antarctic ice temperatures in Fig. (1). The most likely explanation is the diffusion of water vapor to the Antarctic atmosphere, as a result of the increased capacity for water vapor in warmer global atmosphere[22, 23]. The strong natural greenhouse effect of the additional water vapor would amplify the effect of cloud forcing globally (positive feedback) and over-ride it in Antarctica (negative feedback).

Finally, it is possible to map zonally averaged NASA-GISS temperature data for the past century so that the Antarctic Climate Anomaly become apparent. By removing the linear trend of the 8 zonal temperature bands series covering the years 1903-2005, and subsequently sort all the 8 temporal time series after the descending temperatures of the 64-90 latitude band, Fig. (4b) is obtained. This figure is very similar to Fig. (3), with a saddle point structure in the southern hemisphere. In this case the node of the saddle point seems to be at somewhat lower latitudes. This effect could real and caused by clouds over the ocean. A resent study found that poleward of -58.75 (observational limit) had a heating effect on the surface over most of the year[10].

Cloud forcing is by far the most economical hypothesis that explains the patterns of Fig. (1) and Fig. (4), as well as the bigger see-saw effects in Wurm-Wisconsin times[15]. There is plainly scope for more detailed modeling of the Antarctic climate anomaly on various timescales.

Meanwhile, a chain of evidence appears to be complete, which links low-level clouds to the well-known modulation of galactic cosmic-ray intensity by solar magnetic activity, to the detected influence of galactic cosmic rays on cloudiness[1, 2, 3], and also to experimental evidence that electrons set free by passing muons help to make aerosols the pre-cursor to cloud condensation nuclei at low altitudes[4]. The roles of cosmic rays and clouds as active players in climate change therefore merit closer attention in general climate modeling and in solar and heliospheric physics, with special regard to the high-energy galactic cosmic rays that ionize the lower atmosphere. Physics history comes full circle. More than 100 years

ago, C.T.R. Wilson developed the cloud chamber to try to understand natural clouds but he was diverted by his detection of ionizing particles. In 1937 the first known muons turned up in a cloud chamber[24]. Now Wilson's initial purpose is fulfilled in a fresh understanding of the physics of natural low-level clouds, and in the evidence presented here for its relevance in the real world.

-
- [1] H. Svensmark and E. Friis-Christensen, *JATP*, **59**, 1225, (1997).
 - [2] H. Svensmark, *Phys. Rev. Lett.*, **81**, 5027, (1998).
 - [3] N. D. Marsh and H. Svensmark, *Phys. Rev. Lett.*, **85**, 5004, (2000).
 - [4] H. Svensmark *et al.*, P. Royal. Soc. A (in press).
 - [5] W. Ambach, *J. Glaciol.*, **13**, 73 (1974).
 - [6] N. Nakamura and A. H. Oort, *J. Geophys. Res.*, **93**, 9510 (1988).
 - [7] T. Konzelmann, *et al.*, *Global Planet. Change*, **9**, 143 (1994).
 - [8] R. Bintanja and M.R. Van den Broeke, *Int. J. of Climatology*, **16**, 1281 (1996).
 - [9] M. Nardino, *et al.*, *ECAC 2000, Cloud radiative forcing and effects on local climate*, 3rd European Conference on Applied Climatology, Pisa, Italy, 16-20 October, (2000).
 - [10] M. J. Pavolonis and J. R. Key *Journal of Applied Meteorology*, **42**, 827, (2003).
 - [11] V. Ramanathan, *et al.*, *Science*, **243**, 57 (1989).
 - [12] B. R. Barkstrom, E. F. Harrison, and R. B. Lee, *EOS Transactions, American Geophysical Union*, **71**, February 27 (1990).
 - [13] D. Dahl-Jensen, *et al.*, *Science*, **282**, 268 (1998).
 - [14] D. Dahl-Jensen, V.I Morgan, and A. Elcheikh, *Annals of Glaciology*, **29**, 145 (1999).
 - [15] T. Blunier and E.J. Brook, *Science*, **291**, 109, (2001).
 - [16] N. Shackleton, *Science*, **291**, 58, (2001).
 - [17] R. Knutti, *et al.*, *Nature* **430**, 851, (2004).
 - [18] G. R. North, *J. Atm. Sci.*, **32**, 2033, (1975).
 - [19] P. D. Jones, *et al.*, *Rev. Geophys.*, **37**, 173 (1999).
 - [20] Annual mean Land-Ocean Temperature Index in .01 C selected zonal means sources: GHCN 1880-06/2006 + SST: 1880-11/1981 HadISST1 12/1981-06/2006 Reynolds v2 using elimination of outliers and homogeneity adjustment - base period: 1951-1980. The data can be obtained from: <http://data.giss.nasa.gov/gistemp/taledata/ZonAnn.Ts+dSST.txt>
 - [21] M. Lockwood, R. Stamper, and M. N. Wild, *Nature*, **399**, 437, (1999).
 - [22] D. B. Kirk-Davidoff, *et al.*, *Nature*, **402**, 399, 1999
 - [23] S. L. Jain, *et al.*, *Current Science*, **89**, 1917, (2005).
 - [24] J.C. Street, E.G. Stevenson, *Phys. Rev.* **52**, 1003 (1937).